The histone demethylase KDM5 controls developmental timing in *Drosophila* by promoting prothoracic gland endocycles.

Coralie Drelon[1], Helen M. Belalcazar[1] and Julie Secombe[1,2,3]

[1] Department of Genetics
Albert Einstein College of Medicine
1300 Morris Park Avenue
Bronx, NY, 10461
United States

[2] Dominick P. Purpura Department of Neuroscience
Albert Einstein College of Medicine
1410 Pelham Parkway South
Bronx, NY, 10461
United States

[3] corresponding author: julie.secombe@einstein.yu.edu

Running title: Larval growth regulation by the histone demethylase KDM5

Key words: KDM5, Lid, transcription, prothoracic gland, endocycle, Torso, Cyclin E, growth control

Summary

Across species, animal growth and maturation are achieved through the production and integration of hormonal signals. However, the molecular mechanisms underlying the transcriptional regulation of these processes remain largely uncharacterized. Here we show that in *Drosophila*, the histone demethylase KDM5 functions in the larval prothoracic gland to control larval growth rate by regulating levels of the steroid hormone ecdysone. Specifically, KDM5 functions in prothoracic gland cells by promoting their endoreplication, a process that increases ploidy and is rate-limiting for the expression of ecdysone biosynthetic genes. We propose that KDM5 regulates the expression of the receptor tyrosine kinase *torso* and that this in turn promotes prothoracic cell polyploidization and growth through activation of the MAPK signaling pathway and expression of the cell cycle regulator Cyclin E. Together, our studies provide key insights into the biological processes regulated by KDM5 and the molecular mechanisms that govern the transcriptional regulation of larval growth.

INTRODUCTION

Covalent modifications to nucleosomal histone proteins that comprise chromatin is one key means by which transcription is regulated (Bannister and Kouzarides, 2011). The enzymes that add or remove these modifications play critical roles during development and their dysregulation can lead to disease states (Mirabella et al., 2016). Lysine demethylase 5 (KDM5) family proteins are chromatin-mediated regulators of transcription that are encoded by four paralogous genes in mammalian cells, KDM5A-D, and by a single gene in *Drosophila*, *kdm5* (also known as *little imaginal discs*; *lid*). The most well-established gene regulatory function of KDM5 proteins is their enzymatic activity that demethylates trimethylated lysine 4 of histone H3 (H3K4me3) (Accari and Fisher, 2015; Xhabija and Kidder, 2018). High levels of H3K4me3 are found surrounding transcriptional start sites and correlate with active gene expression (Santos-Rosa et al., 2002). While absolute levels of H3K4me3 are unlikely to be primary drivers of gene expression levels, the breadth of these promoter peaks can impact transcriptional consistency (Benayoun et al., 2014; Howe et al., 2017). Recruitment of KDM5 to promoters to demethylate H3K4me3 is therefore one mechanism by which this family of proteins regulate transcription. KDM5 proteins can also affect gene expression through demethylase-independent mechanisms, such as by through interactions with the chromatin remodeling NuRD complex or by affecting histone acetylation by interacting with lysine deacetylase (HDAC) complexes (Barrett et al., 2007; Gajan et al., 2016; Lee et al., 2009; Liu et al., 2014; Nishibuchi et al., 2014).

KDM5 proteins play key roles in orchestrating diverse gene expression programs. This is emphasized by the large volume of literature linking the dysregulation of KDM5 proteins to two seemingly disparate diseases, cancer and intellectual disability. Whole exome sequencing of patients with intellectual disability has identified loss of function mutations in KDM5A, KDM5B and KDM5C (Collins et al., 2019; Kim et al., 2017; Vallianatos and Iwase, 2015). Efforts to understand the basis of link between KDM5 and intellectual disability using mice, flies and

worms have revealed that KDM5 regulates many genes that could impact neuronal function. These include genes that encode synaptic components, mediate axonal growth, constituents of learning and memory pathways and proteins involved in regulating gut-microbiome-brain interactions (Chen et al., 2019; Iwase et al., 2016; Mariani et al., 2016; Zamurrad et al., 2018). However, the extent to which any of these pathways contribute to cognitive impairment observed in patients remains unknown. A similar deficit exists in our understanding of how the dysregulation of human KDM5 genes leads to a range of cancer types (Blair et al., 2011; Plch et al., 2019). Unlike intellectual disability that is exclusively associated with loss of function mutations in KDM5 genes, malignancies are associated with overexpression of KDM5A or KDM5B, either loss or gain of KDM5C, or loss of KDM5D. The best studied of these is the overexpression of KDM5B observed in breast cancer and melanoma that correlates with poor prognosis (Han et al., 2017). Despite being shown to directly or indirectly regulate genes involved in cell cycle progression, cancer stem cell survival and DNA repair, no clear model has emerged to explain its oncogenic capacities (Catchpole et al., 2011; Han et al., 2017; McCann et al., 2019; Roesch et al., 2013; Yamamoto et al., 2014; Yamane et al., 2007). Our lack of understanding of KDM5-regulated pathways that lead to disease states underscores the importance of defining the physiological functions of KDM5 proteins.

Drosophila melanogaster offers an ideal genetically amenable model to provide fundamental insights into KDM5 function *in vivo*, as it encodes a single, highly conserved, *kdm5* gene (Gildea et al., 2000). Moreover, in contrast to viable knockouts of KDM5A, KDM5B or KDM5C in mice, loss of *Drosophila* KDM5 results in lethality (Albert et al., 2013; Drelon et al., 2018; Iwase et al., 2016; Klose et al., 2007; Martin et al., 2018). This allows us to dissect critical functions of KDM5 without the complication of functional redundancy between mammalian KDM5 paralogs that could partially occlude phenotypes. Using *Drosophila*, we have previously shown that *kdm5* null mutants take 5 days longer than wild-type animals to complete larval development, linking

KDM5 function to growth control. Interestingly, this phenotype is independent of the histone demethylase activity of KDM5, as animals specifically lacking this enzymatic function grow normally and produce viable adult flies (Drelon et al., 2018; Li et al., 2010). Emphasizing the importance of understanding cellular functions of KDM5 proteins that are independent of their enzymatic activity, the contribution of KDM5's demethylase function to normal development and to disease states in mammalian cells remains unresolved. For instance, while some intellectual disability-associated mutations in KDM5C reduce *in vitro* histone demethylase activity, others do not (Brookes et al., 2015; Iwase et al., 2007; Tahiliani et al., 2007; Vallianatos et al., 2018). Similarly, whereas the growth of some cancers can be attenuated by pharmacologically inhibiting KDM5 activity, KDM5 appears to act through demethylase-independent activities in others (Cao et al., 2014; Paroni et al., 2018). KDM5 proteins are therefore likely to utilize more than one gene-regulatory activity to control a range of cellular processes *in vivo.*

Here we demonstrate that KDM5 regulates larval development by playing an essential role in the prothoracic gland, a tissue that secretes the steroid hormone ecdysone, which is a key regulator of animal growth and maturation (Yamanaka et al., 2013). Indeed, although KDM5 is expressed ubiquitously during larval development, re-expression of *kdm5* exclusively in the prothoracic gland within a *kdm5* null mutant background rescues the larval growth delay and restores adult viability. We further show that within cells of the prothoracic gland, KDM5 is necessary to promote the endoreplicative cell cycles that increase DNA copy number and is required for the transcription of enzymes that mediate ecdysone production (Ohhara et al., 2017). This effect is likely to be achieved through regulation of the Torso receptor tyrosine kinase by KDM5. While stimulation of the Torso receptor and subsequent activation of the MAPK pathway is known to be necessary for ecdysone production (Rewitz et al., 2009), it has not been previously linked to either KDM5, nor to the regulation of prothoracic gland

endocycles. Our data therefore provide new insights into the molecular mechanisms underlying the regulation of ecdysone production and developmental growth control.

RESULTS:

KDM5 expression in the prothoracic gland is sufficient to rescue lethality and restore correct developmental timing to *kdm5* null mutants.

To understand the underlying basis of the lethality caused by the $kdm5^{140}$ null allele, we sought to define the spatial requirements of KDM5 during development. To do this, we re-expressed *kdm5* in a null mutant background using a UAS-inducible transgene we have previously used to rescue hypomorphic alleles of *kdm5* (Li et al., 2010) (Table 1). Ubiquitous expression of this UAS-*kdm5* transgene using Ubiquitin-Gal4 (Ubi-Gal4) resulted in slightly higher than endogenous levels of KDM5 expression and rescued the lethality of $kdm5^{140}$ to produce morphologically normal adult flies (Figure 1A, B; Table 1). Re-expressing *kdm5* ubiquitously also led to a developmental timing profile that was indistinguishable from wild-type flies (Figure 1C). This is consistent with the observation by us and others that KDM5 is broadly expressed in all cell types examined to-date (Lee et al., 2009; Liu et al., 2014; Moshkin et al., 2009; Secombe et al., 2007; Tarayrah et al., 2015; Zamurrad et al., 2018).

To test whether KDM5 plays key developmental roles in specific tissues, we tested a range of Gal4 drivers for their ability to rescue $kdm5^{140}$ lethality when combined with UAS-*kdm5* (Table 1). These included strains that drive Gal4 expression in tissues that have phenotypes in *kdm5* mutant or knockdown larvae such as imaginal discs and hemocytes (Drelon et al., 2018; Moran et al., 2015; Moshkin et al., 2009). In addition, we tested tissues linked to the regulation of larval growth such as the hormone-producing larval prothoracic gland, insulin secreting cells of the brain, or cells of the fat body that coordinate larval growth with feeding and nutritional status (Yamanaka et al., 2013). Significantly, all Gal4 drivers that were expressed in the larval

prothoracic gland significantly rescued *kdm5*^{140} lethality, including spookier-Gal4 (spok-Gal4), which is expressed exclusively in this tissue (Table 1) (Hrdlicka et al., 2002; Moeller et al., 2017; Shimell et al., 2018). Consistent with KDM5 playing critical functions in the larval prothoracic gland that secretes the steroid hormone ecdysone, spok-Gal4-mediated re-expression of *kdm5* was sufficient to rescue the developmental delay of *kdm5*^{140} (Figure 1C).

Similar to Ubi-Gal4-mediated rescue of *kdm5*^{140}, adult flies generated by re-expression of *kdm5* in the prothoracic gland such as spok-Gal4 were wild-type size but had wings that were curved downward (Figure 1B). KDM5 is therefore important for wing development, however this activity is not essential for viability. A similar curved-down wing phenotype was observed in *kdm5*^{140} flies that expressed *kdm5* in the wing imaginal disc in addition to the prothoracic gland such as Mai60-Gal4 or 32B-Gal4, but not with the more broadly expressed T80-Gal4 driver (Figure 1B, Table 1). The expression of these imaginal disc Gal4 drivers after larval development is not known, thus the wing defect observed could be due to a requirement for KDM5 during pupal development or during wing maturation in newly eclosed flies (Table 1). In addition, while expression of *kdm5* in the prothoracic gland allowed *kdm5*^{140} mutant pupae to eclose, adult flies were shorter-lived than flies expressing *kdm5* ubiquitously (Figure 1D; $P<0.0001$). It is also noteworthy that while adults rescued by ubiquitous expression of *kdm5* were largely male and female fertile, prothoracic gland re-expression of *kdm5* resulted in significant infertility (Table 2). These data are consistent with previous observations showing roles for KDM5 in oogenesis and in testis germline stem cell proliferation (Navarro-Costa et al., 2016; Tarayrah et al., 2015; Zhaunova et al., 2016). Together, these studies demonstrate essential roles for KDM5 in the larval prothoracic gland and in other cell types that are important for wing maturation, adult survival and reproduction.

Loss of KDM5 affects proliferation and cell death in wing imaginal discs non-cell-autonomously.

We previously showed that wing imaginal discs from *kdm5*^{140} mutant larvae have decreased proliferation as assessed by quantifying phosphorylated histone H3 levels (Figure 2A) (Drelon et al., 2018). As expected, re-expressing *kdm5* ubiquitously using Ubi-Gal4 restored levels of pH3 to wild-type levels (Figure 2B, C). To test the cell autonomy of this defect, we examined *kdm5* mutant animals expressing *kdm5* under the control of Mai60-Gal4 and spok-Gal4. Consistent with their known expression patterns, Western blot analyses showed that Mai60-Gal4 resulted in wing imaginal disc expression of KDM5 that was slightly lower than wild-type, whereas spok-Gal4 did not drive any detectable KDM5 expression (Figure 2B). Examining levels of wing disc pH3 in larvae re-expressing *kdm5* using Mai60-Gal4 or spok-Gal4 revealed that levels of this mitotic marker were rescued to wild-type levels (Figure 2B, C). The reduced proliferation observed in *kdm5*^{140} wing discs is therefore likely to be an indirect consequence of defective prothoracic gland function.

Because *kdm5*^{140} wing imaginal discs also showed an increased number of apoptotic cells as shown by using an antibody that detects the cleaved caspase Dcp-1, we examined the basis for this phenotype (Drelon et al., 2018). Similar to our analyses of pH3, the increased number of Dcp-1 positive cells seen in *kdm5*^{140} wing discs was restored to wild-type by expressing *kdm5* using Mai60-Gal4 or spok-Gal4 (Figure 2D-I). Thus, neither the proliferative nor the apoptotic phenotypes of *kdm5*^{140} wing imaginal discs were caused by loss of KDM5 in the disc itself. Interestingly, these data show that the curved wing phenotype observed in adult flies rescued by prothoracic expression of *kdm5* is not caused by wing imaginal disc proliferative or cell death phenotypes. This is in keeping with the prediction that this defect is due to a requirement for KDM5 during pupal development or early adulthood (Table 1).

Reduced ecdysone production causes the developmental delay of *kdm5^{140}* mutant larvae.

The prothoracic gland, corpus allatum and corpora cardiaca are the three sub-tissues that comprise the larval ring gland, a semi-circular structure associated with the central larval brain. Each of these sub-tissues types produces a different hormone that regulates larval development or metabolism (Yamanaka et al., 2013). Whereas the prothoracic gland synthesizes ecdysone, the corpus allatum and corpora cardiaca produce juvenile hormone and adipokinetic hormone, respectively. Because juvenile hormone acts in concert with 20E to trigger larval-larval molts, we tested whether expressing *kdm5* in the corpus allatum rescued the lethality of *kdm5^{140}* using *Aug21*-Gal4 (Gaziova et al., 2004) (Table 1). In contrast to expression in the prothoracic gland, no significant rescue was observed when *kdm5* was reintroduced in the corpus allatum. Similarly, expression of *kdm5* in the corpora cardiaca using Akh-Gal4 failed to rescue *kdm5^{140}* mutants (Lee and Park, 2004) (Table 1). Thus, within the ring gland, KDM5 is critical only for prothoracic gland function, linking its transcriptional regulatory functions to ecdysone biology.

Based on the requirement for KDM5 in the prothoracic gland, we tested whether levels of ecdysone were reduced in *kdm5^{140}* larvae by quantifying the amount the active form of this hormone (20-hydroxyecdysone; 20E) in whole 3rd instar larvae. These analyses revealed that *kdm5^{140}* larvae had a 3-fold reduction in 20E levels and concomitant reduction in the expression of ecdysone-regulated genes such as *broad*, *E74* and *E75* (Figure 3A, B). Ecdysone is synthesized in the prothoracic gland from cholesterol through the action of a series of cytochrome p450 biosynthetic enzymes that include *neverland* (*nvd*), *spookier* (*spok*) and *disembodied* (*dib*) (Gilbert, 2004). It is then subsequently converted to 20E in larval cells by the hydroxylase Shade (*shd*). qPCR analyses to examine the expression of these genes revealed that *nvd*, *spok* and *dib* transcripts were significantly decreased in *kdm5^{140}* mutant 3rd instar larvae, while levels of *shd* mRNA were unchanged (Figure 3C, D). *kdm5^{140}* mutants therefore have reduced 20E due to a defect in the biosynthesis of ecdysone in the prothoracic gland.

To test whether re-expression of *kdm5* in the prothoracic gland was sufficient to restore ecdysone production, we quantified levels of 20E in $kdm5^{140}$ animals expressing UAS-*kdm5* using Ubi-Gal4, Mai60-Gal4 or spok-Gal4. All three Gal4 drivers restored levels of 20E, the expression of ecdysone-regulated genes, and transcription of the ecdysone biosynthetic genes *nvd, spok* and *dib* to wild-type (Figure 3A-D). Based on these data, dietary supplementation with 20E would be expected to attenuate the developmental delay caused by loss of KDM5. To test this, we fed wild-type and $kdm5^{140}$ larvae food containing 20E or vehicle alone (ethanol) as a control. As shown in Figure 3E, exogenously providing 20E rescued the developmental delay of *kdm5* mutant larvae, emphasizing the importance of KDM5-mediated regulation of ecdysone production.

KDM5 is required for prothoracic gland growth by regulating the Torso signaling pathway.

During larval development, cells of the prothoracic gland undergo endoreplicative cycles in the absence of mitosis that increases their DNA content up to ~64C (Aggarwal and King, 1969). These endocycles are required for maximal expression of the genes that synthesize ecdysone (Ohhara et al., 2017). To test whether *kdm5* mutants show an endocycle defect, we quantified the number of prothoracic gland cells undergoing S-phase by incorporating the thymine nucleoside analog 5-ethynyl-2'-deoxyuridine (EdU). This revealed a significant decrease in the number of EdU positive cells in $kdm5^{140}$ prothoracic glands compared to wild-type (Figure 4A-I). Importantly, loss of KDM5 caused these endocycle defects without altering the total number of cells that comprise the prothoracic gland (Figure 4J). Prothoracic gland cell specification therefore occurs normally during embryogenesis in *kdm5* mutants, however the cells fail to endocycle and grow correctly during larval development. Overexpression of the G1-S phase cell cycle regulator Cyclin E in the prothoracic gland can bypass a starvation-induced block to

endoreplication (Ohhara et al., 2017). Based on this, we expressed a UAS-*cyclin E* transgene in *kdm5*^{140} mutant larvae using spok-Gal4 and found that this was sufficient to rescue larval developmental timing (Figure 4K). A deficit in prothoracic gland cell endocycling is therefore likely to be a key cause of the developmental delay seen in *kdm5*^{140} larvae.

To further explore the mechanism by which KDM5 affects developmental timing upstream of Cyclin E, we examined the activity of the insulin and the Torso/MAPK pathways, as these are known regulators of ecdysone production (Yamanaka et al., 2013). Activation of the insulin receptor by insulin-like peptides leads to the phosphorylation of Akt which subsequently induces cell growth and endocycling through the target of rapamycin (TOR) pathway (Danielsen et al., 2016; Ohhara et al., 2017). Ecdysone production is also regulated by activation of the Torso receptor by prothoracicotropic hormone (PTTH), which then induces a Ras/ERK MAP kinase cascade that leads to ecdysone production (Niwa and Niwa, 2014; Yamanaka et al., 2013). To test whether these pathways were altered in *kdm5* mutant larvae, we examined levels of phosphorylated Akt and ERK as surrogates for the activity of the insulin and Torso pathways, respectively. Western blot analyses of *kdm5*^{140} ring glands showed that while levels of phosphorylated Akt was unaffected, phosphorylation of ERK was decreased 2-fold (Figure 5A-C). Because ERK is phosphorylated in response to activation of the Torso receptor, we next quantified mRNA levels of the *torso* receptor and found that they were significantly decreased in *kdm5*^{140} (Figure 5D). The reduced levels of activated ERK and downstream defects in prothoracic gland endocycling could therefore be due to defective *torso* expression. Consistent with this model, expression of this receptor in the prothoracic gland using a UAS-*torso* transgene rescued the developmental delay of *kdm5*^{140} mutants (Figure 5E). Reduced Torso signaling and subsequent slowing of endocycling through Cyclin E could therefore mediate the developmental delay caused by loss of KDM5 (Figure 5F).

Discussion

Here we demonstrate that KDM5 is essential for the function of the ecdysone-producing prothoracic gland during *Drosophila* larval development. Critical to this conclusion was our finding that expressing *kdm5* in the prothoracic gland was sufficient to rescue the lethality and developmental delay phenotypes of $kdm5^{140}$ null allele homozygous mutant animals. Consistent with this observation, prothoracic gland function was defective in *kdm5* mutants, with mutant larvae having low levels of ecdysone and reduced expression of downstream hormone-responsive target genes. Demonstrating the importance of KDM5-mediated regulation of ecdysone production, dietary supplementation of 20E restored normal developmental timing to *kdm5* mutant larvae. At the cellular level, loss of KDM5 slowed the prothoracic gland endoreplicative cycles that increase the ploidy of these cells and are key to ecdysone biosynthesis (Ohhara et al., 2017). Restoring these endocycles by overexpressing *cyclin E* or the upstream receptor tyrosine kinase *torso* reestablished normal developmental timing to $kdm5^{140}$ mutants. Thus, we propose that KDM5-mediated activation of the Torso pathway is essential for normal larval development.

We propose that one key function of KDM5 is to regulate the expression of the *torso* gene, reduction in which lowers signaling through the MAPK pathway, slows the endocycling of prothoracic gland cells and delays larval development. Consistent with this, mutations in *torso*, or ablation of the neurons that produce its ligand PTTH, cause a 5-day delay to larval development similar to that observed for $kdm5^{140}$ (Drelon et al., 2018; McBrayer et al., 2007; Rewitz et al., 2009). Very little known is about the transcriptional regulation of *torso* and other genes that comprise the pathways that mediate ecdysone production. One possibility is that KDM5 is a direct transcriptional activator of the *torso* gene, thus decreased expression of this receptor would be expected in *kdm5* mutant animals. Because of the small size of the prothoracic gland, it is not currently feasible to carry out ChIP experiments to examine KDM5

promoter binding in this tissue. It is, however, notable that the promoter of *torso* was not bound by KDM5 in existing ChIP-seq datasets from the larval wing imaginal disc or from whole adult flies (Liu and Secombe, 2015; Lloret-Llinares et al., 2012). This could be because *torso* expression is largely restricted to the prothoracic gland during larval development and so may not be expected to have promoter-bound KDM5 in the tissues examined to-date (Rewitz et al., 2009). Alternatively, KDM5 might regulate *torso* indirectly. In the silkworm *Bombyx mori*, expression of the *torso* gene is repressed in response to starvation conditions (Gu et al., 2011). Although the mechanism by which this occurs is unknown, it does indicate that other cellular defects caused by loss of KDM5 could lead to changes to *torso* transcription and subsequent decrease in ecdysone production. Whether the regulation of *torso* by KDM5 is direct or indirect, it occurs in a demethylase-independent manner, as larvae lacking enzymatic activity show a normal developmental profile (Drelon et al., 2018). Consistent with this observation, components of KDM5 complexes that regulate gene expression through demethylase-independent mechanisms also affect developmental timing. For example, a development delay similar to that of $kdm5^{140}$ is caused by RNAi-mediated knockdown of the histone deacetylase *HDAC1* or the NuRD complex components *asf1* and *Mi-2* (Danielsen et al., 2016). KDM5 could therefore interact with these proteins to regulate the expression of genes critical to the regulation of larval development.

Based on the ability of *cyclin E* or *torso* expression to rescue the developmental timing of *kdm5* mutant larvae, we propose that these two genes lie in the same KDM5-regulated pathway. While the Torso pathway is known to regulate ecdysone by activating the expression of ecdysone biosynthetic genes (Danielsen et al., 2013; Rewitz et al., 2009), it has not been linked to the regulation of the prothoracic gland endocycles. However, recent data demonstrating that increased ploidy within the cells of the prothoracic gland is necessary for the expression of these genes is entirely consistent with our model (Ohhara et al., 2017). Indeed,

because steroidogenic genes are among the most abundantly expressed gene in the prothoracic gland, their expression level may be entirely limited by gene copy number (Christesen et al., 2017; Fox and Duronio, 2013). A similar requirement for copy number amplification to produce optimal gene expression levels has been observed in other cell types in *Drosophila*, including chorion gene expression in ovarian follicle cells (Orr-Weaver, 2015). How could Torso/MAPK activation promote prothoracic gland cell cycle progression? One possibility is through the transcription factor E2f1, which is essential for both mitotic and endoreplicative cell cycles (Davoli and de Lange, 2011; Fox and Duronio, 2013; Frawley and Orr-Weaver, 2015). This model is based on studies of the polyploid enterocytes of the adult midgut, in which activation of the MAPK pathway via the EGF receptor stabilizes E2f1 protein, leading to transcription activation of *cyclin E* (Xiang et al., 2017). Alternatively, it is possible that the effect of KDM5 on prothoracic gland endocycles is not downstream of the canonical Torso pathway. Cyclin E expression in the prothoracic gland can be regulated by activation of the insulin receptor and the TORC1 complex (Ohhara et al., 2017). While it remains largely uncharacterized, there is likely to be cross-talk between the Torso and insulin pathways in order to integrate extrinsic and intrinsic signals and coordinate ecdysone production. Genetic dissection of where KDM5 lies with respect to established components of the Torso and TOR pathways will provide clarity on this important issue.

Our observed role of KDM5 in the growth and polyploidization of larval prothoracic gland cells raises the possibility that this transcriptional regulator might play a role in other cell types that utilize endoreplicative cycles. This could have broad consequences for our understanding of KDM5 biology, since polyploidization is observed in many plant and animal cell types and is widely used during *Drosophila* larval development (Fox and Duronio, 2013; Orr-Weaver, 2015). For example, polyploid cells of the larval fat body survive until early adulthood where they necessary for survival because flies are unable to immediately begin feeding (Aguila et al.,

2007). In fact, a role for KDM5 in cells of the fat body would provide an explanation for the shortened adult lifespan of *kdm5* mutant flies rescued by prothoracic gland-specific expression of *kdm5*. In addition to being critical for normal development, endocycling cells are also found in tumors in both humans and *Drosophila* (Cong et al., 2018; Davoli and de Lange, 2011; Fox and Duronio, 2013). While the role of polyploid cells in the etiology or maintenance of cancers remains a topic of ongoing research, KDM5-regulated endocycling could contribute to its tumorigenic activities in humans. Regulation of polyploidization the nervous system could also contribute to the role of KDM5 proteins in intellectual disability (Vallianatos and Iwase, 2015). This could, for instance, be mediated by KDM5 function in glial cells, as polyploidization of a superineurial glial cells in *Drosophila* is required for normal brain development (Unhavaithaya and Orr-Weaver, 2012). While it is not clear the extent to which a similar phenomenon occurs during human brain development, it is interesting to note that glial cell types contribute to the clinical severity of intellectual disability disorders such as Rett syndrome (Sharma et al., 2018). Thus, while there is still much to be learned regarding the contribution of polyploid cells to normal development and to disease states, KDM5-regulated transcriptional programs are likely to be important in cells that utilize this variant cell cycle.

Acknowledgements

We would like to thank members of the Secombe and lab for insights at all stages of this project. We are very grateful for fly strains generously donated by Michael O'Connor and Helena Richardson in addition to the Bloomington Drosophila Stock Center (NIH P400D018537). The 12G10 monoclonal antibody was obtained from the Developmental Studies Hybridoma bank, created by the NICHD of the NIH and maintained at The University of Iowa. We also thank the NIH (R01 GM112783) and the Einstein Cancer Center Support Grant P30 CA013330.

Author Contribution

Conceptualization, J.S., C.D. and H.B.; Methodology C.D, and H.B.; Investigation, C.D. and H.B.; Writing – original draft, J.S., Writing – Reviewing and Editing, J.S., C.D. and H.B.; Funding acquisition, J.S., Supervision, J.S.

Declaration of Interests

The authors declare no competing interests.

Figure 1: KDM5 expression in the prothoracic gland rescues *kdm5^{140}* developmental delay and lethality

(A) Western blot using 3rd instar larval wing imaginal discs (five per lane) from wild-type, *kdm5^{140}* and *kdm5^{140}* expressing *kdm5* ubiquitously (*kdm5^{140}* ; Ubi>*kdm5*). Anti-KDM5 (top) is indicated by the arrowhead. Anti-alpha-tubulin is used as a loading control (bottom).

(B) Male wild-type fly (*kdm5^{140}* ; g[*kdm5*:HA]attp86F).

(B') Male *kdm5^{140}*, Ubi>*kdm5* adult fly showing morphologically normal features.

(B'') Male *kdm5^{140}* ; Mai60>*kdm5* adult fly with normal body and slightly curved wings indicated by arrow.

(B''') Male *kdm5^{140}* ; spok>*kdm5* adult fly with normal body and curved wings indicated by arrow.

(C) Number of days taken for pupariation to occur in wild-type, *kdm5^{140}* , *kdm5^{140}* ; Ubi>*kdm5*, *kdm5^{140}* ; *Mai60>kdm5* and *kdm5^{140}* ; *spok>kdm5.*

(D) Adult survival for *kdm5^{140}* ; Ubi>*kdm5* (N=56)*, kdm5^{140}* ; Mai60>*kdm5* (N=62)and *kdm5^{140}* ; spok>*kdm5* (N=51) rescued male flies. Mai60 and spok-Gal4-rescued flies are significantly shorter lived than Ubi-Gal4-rescued flies (Mantel-Cox log-rank test; P<0.0001).

Figure 2: Increased cell death and reduced proliferation in *kdm5^{140}* wing discs is due to non-cell autonomous effects.

(A) Western blot using anti-KDM5 (top), anti-phophorylated histone H3 (middle; pH3) and total histone H3 (bottom; H3) in wild-type and *kdm5^{140}* wing discs. Six wing discs per lane.

(B) Western blot using wing discs from *kdm5^{140}* mutants re-expressing *kdm5* using Ubi-Gal4, Mai60-Gal4 or spok-Gal4. anti-KDM5 (top), pH3 (middle) and total H3 (bottom). Six wing discs per lane.

(C) Quantification of the levels of pH3 relative to total H3 from three Western blots. ** P <0.01 (one-way ANOVA). Error bars indicate SEM.

(D) Wild-type wing imaginal disc from wandering 3rd instar larva stained with anti-Dcp-1. Dotted circle indicates pouch region of the wing disc that was used to count Dcp-1 positive cells.

(E) *kdm5*^{140} mutant wing imaginal disc stained with the apoptosis marker anti-Dcp-1.

(F) Anti-Dcp-1 staining of a wing imaginal disc from *kdm5*^{140} mutant re-expressing *kdm5* in imaginal discs and prothoracic gland using Mai60-Gal4 (*kdm5*^{140} ; Mai60>*kdm5*).

(G) Anti-Dcp-1 staining of a wing imaginal disc from *kdm5*^{140} mutant re-expressing *kdm5* in the prothoracic gland with spok-Gal4 (*kdm5*^{140} ; spok>*kdm5*).

(H) Quantification of the number of Dcp-1 positive cells in the pouch region of wing imaginal discs from wild-type, *kdm5*^{140}, *kdm5*^{140} ; Ubi>*kdm5, kdm5*^{140} ; Mai60>*kdm5 and kdm5*^{140} ; spok>*kdm5. ****P<0.0001, ***P<0.001, *P<0.05* (one-way ANOVA). Error bars indicate SEM.

Figure 3: Exogenous ecdysone rescues the developmental delay of *kdm5*^{140} mutants.

(A) Quantification 20E levels in pg per larva using wild-type, *kdm5*^{140}, *kdm5*^{140} ; Ubi>*kdm5*, *kdm5*^{140} ; Mai60>*kdm5* and *kdm5*^{140} ; spok>*kdm5* whole 3rd instar larvae. **** P<0.001 (one-way ANOVA). Error bars indicate SEM.

(B) Real-time PCR quantifying the mRNA levels of the ecdysone target genes *broad*, *E74* and *E75* in *kdm5*^{140} , *kdm5*^{140} ; Ubi>*kdm5*, *kdm5*^{140} ; Ma60>*kdm5* and *kdm5*^{140} ; spok>*kdm5* whole larvae. Data were normalized to *rp49* and shown relative to wild-type. * P<0.05, **P<0.01, ***P<0.001. Error bars indicate SEM.

(C) Real-time PCR showing mRNA levels *nvd*, *spok* and *dib* from whole 3rd instar wild-type, *kdm5*^{140} ; Ubi>*kdm5*, *kdm5*^{140} ; Mai60>*kdm5* and *kdm5*^{140} ; spok>*kdm5* larvae. Data were normalized to *rp49* and shown relative to wild-type. Error bars indicate SEM.

(D) Real-time PCR showing mRNA levels of the hydroxylase *Shade* from whole 3rd instar wild-type, *kdm5*^{140} ; Ubi>*kdm5*, *kdm5*^{140} ; Mai60>*kdm5* and *kdm5*^{140} ; spok>*kdm5* larvae. Data were normalized to *rp49* and shown relative to wild-type. Error bars indicate SEM.

(E) Quantification of the time for pupariation to occur upon feeding 20E to wild-type (N=103) and *kdm5*^{140} (N=62) or vehicle alone (ethanol) to wild-type (N=67) or *kdm5*^{140} (N=60).

Figure 4: *kdm5*^{140} larvae have a prothoracic gland endocycle defect.

(A-D) Control flies in which EdU incorporation was carried out using larvae from a cross of spok>GFP to the wild-type strain *w*^{1118} to mark prothoracic gland cells. (A) GFP (B) EdU (C) dapi (D) merge of EdU and GFP channels.

(E-H) EdU incorporation into *kdm5*^{140} mutant larvae carrying spok>GFP to mark cells of the prothoracic gland. (E) GFP (G) EdU (G) dapi (H) merge of EdU and GFP channels.

(I) Quantification of the number of EdU positive prothoracic gland nuclei from control spok>GFP larvae (N=7 larvae) and *kdm5*^{140} homozygyous mutant larvae (N=10) carrying spok>GFP. * P<0.05 (Student's t-test). Error bars indicate SEM.

(J) Quantification of the total prothoracic gland cell number in control spok>GFP (N=12 larvae) and *kdm5*^{140} ; spok>GFP (N=18) larvae. Error bars indicate SEM. ns not significant (Student's t-test).

(K) Quantification of the time for pupariation to occur in wild-type (N=91), *kdm5*^{140} (N=56), *kdm5*^{140} ; spok>*kdm5* (N=73) and *kdm5*^{140} ; spok>*cyclin E* (N=48) animals.

Figure 5: Levels and activity of the Torso receptor pathway are reduced in *kdm5*^{140}.

(A) Western blot from wild-type and *kdm5*^{140} ring glands showing levels of phosphorylated Akt and total Akt as a control. Six rings glands per lane.

(B) Western blot analyses of dissected ring glands from wild-type and *kdm5*^{140} examining levels of phosphorylated ERK (pERK; top) and total ERK (bottom). Five ring glands per lane.

(C) Quantitation of the ratio of pERK to total ERK in *kdm5*^{140} compared to wild-type from three Western blots. **P<0.01 (Student's t-test). Error bars indicate SEM.

(D) Real-time PCR quantitation showing average of biological triplicate of torso mRNA levels from dissected brain-ring gland complexes from wild-type and *kdm5*^{140}. ** P=0.0026 (Student's t-test). Error bars indicate SEM.

(E) Number of days taken for pupariation to occur for wild-type (N=87) *kdm5*^{140} (N=46), *kdm5*^{140} ; spok>*kdm5* (N=57) and *kdm5*^{140} ; spok>*torso* (N=73) animals.

(F) Model for KDM5 function in the prothoracic gland.

Table 1: Re-expressing *kdm5* in defined tissues in *kdm5*^{140} mutants.

Gal4 driver strain	Expression pattern of Gal4 driven expression of KDM5	% of expected flies	Number of flies scored	Significant rescue of lethality?	Adult phenotype of rescued flies?
No Gal4	None	0	300	-	-
Ubiquitin-Gal4	Ubiquitous	83.5%	365	P=8.8e-15	Wild-type
32B-Gal4	Wing imaginal disc Salivary gland Eye-antennal disc Prothoracic gland	21.5%	181	P=6.8e-6	Curved wings
T80-Gal4	Prothoracic gland Imaginal discs Muscle Salivary gland Larval brain Gut	77%	132	P=3.8e-15	Wild-type
Mai60-Gal4	Prothoracic gland Larval brain Imaginal disc	62%	246	P=2.3e-15	Curved wings
spok-Gal4	Prothoracic gland	39%	173	P=2.8e-9	Curved wings
phm-Gal4	Prothoracic gland Leg and wing discs Trachae	44.5%	246	P=1.4e-11	Curved wings
CG-Gal4	Fat body Hemocytes Lymph gland	0%	125	ns P=1	n.a.
dilp2-Gal4	Insulin secreting cells of brain	1.5%	208	ns P=1	n.a.
Mef2-Gal4	Somatic, visceral and cardiac muscle	0%	449	P=1	n.a.
D42-Gal4	Motor neurons Salivary gland	0%	222	P=1	n.a.
Aug21-Gal4	Corpus allatum Salivary gland Tracheae Malpighian tubules Tv neurons	2%	173	ns P=0.5	n.a.
Akh-Gal4	Corpus cardiaca	0%	139	ns P=1	n.a.

Rescue of *kdm5*^{140} lethality using the Gal4 drivers shown in the table shown as a percentage of the number of homozygous mutant *kdm5* flies expected based on Mendelian ratios. Significance determined using Fisher's exact test. n.a. not applicable.

Table 2: Fertility of *kdm5*^{140}-rescued adult flies

Gal4 driver strain	% of fertile female flies	% of fertile male flies
Ubi-Gal4	82% (N=17)	79% (N=19)
Mai60-Gal4	7% (N=14) P=3.8e-05	0% (N=14) P=6e-06
spok-Gal4	0% (N=9) P=7e-05	0% (N=17) P=7.2e-07

Fertility of *kdm5*^{140} homozygous mutant male and female flies expressing UAS-*kdm5* under the control of Ubi-Gal4, spok-Gal4 or Mai60-Gal4. P-values were calculated using Fisher's exact test.

Materials and Methods.

Care of fly strains and crosses

Fly crosses were all carried out at 25°C with 50% humidity and a 12-hour light/dark cycle. Food (per liter) contained 18g yeast, 22g molasses, 80g malt extract, 9g agar, 65 cornmeal, 2.3g methyl para-benzoic acid, 6.35ml propionic acid. Sex of dissected larvae for imaginal disc studies were not determined. For Western blot and real-time PCR analyses, the number of male and female larvae were equal across the genotypes examined. For studies comparing wild-type and *kdm5* mutant larvae, we matched animals for developmental stage, and not chronological age, as we have done previously (Drelon et al., 2018). Thus, wild-type wandering 3rd instar larvae were ~120 hours after egg laying, while *kdm5*^{140} larvae were ~10 days old.

Real-time PCR

Total RNA was purified from either whole larvae or dissected brain-ring gland complexes using TRIzol. Reverse transcription was carried out using 1 μg of RNA (or 5 μg of RNA for ecdysone biosynthetic genes) using a Verso cDNA kit (Thermo-Fisher AB1453A). Real-time PCR used the Power SYBR Green Master Mix and was performed in Applied Biosystems Step ONE plus real-time PCR system**.** Changes to gene expression were determined by normalizing samples to *rp49* (*RpL32*).

Western blot

Western blots were carried out with dissected wing discs or ring glands. Samples were dissected in 1xPBS and transferred to 1xNuPAGE LDS sample buffer, run on a 4-12% Bis-Tris 1mm gel and transferred to PVDF. Secondary antibodies were donkey anti-mouse IgG 680RD

or donkey anti-rabbit IgG 800CW. Blots were scanned using a LI-COR Odyssey Infrared scanner and quantified using LI-COR imaging software v3.0.

Immunostaining of wing discs

Third instar wing imaginal discs were dissected in 1xPBS and fixed in 4% paraformaldehyde for 30 minutes. After blocking in 0.1% BSA/TBST (1xPBS, 0.2% Triton, 0.1% BSA) for 1 hour, samples were incubated with anti-Dcp-1 or anti-pH3 overnight at 4^{o}C. Wing discs were washed with PBST and incubated with anti-rabbit Alexa Fluro 568 secondary antibody for 2 hours at 4^{o}C. Samples were mounted in Vectashield for microscopy.

Edu incorporation into prothoracic glands

For EdU staining, click-IT Edu kit and Alexa Fluor 594 Azide were used. Third instar larvae were dissected in Schneider's *Drosophila* medium and brain-ring gland complexes were in incubated in 50μM EdU in Schneider's Drosophila medium for 2.5 hours at room temperature. After washing in 1xPBS, tissues were fixed in 4% paraformaldehyde for 30 minutes. Tissues were blocked in 3% BSA for 30 minutes and then permeabilized in 0.5% triton and detected using 1x click-IT reaction buffer, CuSO4, Alexa Fluor 594 Azide and reaction buffer additive for 30 minutes. DNA was stained using Hoescht and brain-ring gland complexes were mounted in Vectashield for microscopy.

Larval feeding of 20E

Control wild-type or *kdm5*^{140}/CyO-GFP flies were allowed to mate and lay eggs for 6 hours. At 96 hours AEL, a mixture of dry yeast, 20-hydroxyecdysone (0.33mg/ml in 100% ethanol) or control ethanol alone in 500μl of ddH_2O was added to each vial.

20E quantification

Ecdysone was extracted from whole larvae as previously described (Moeller et al., 2017). Briefly, ten 3rd instar larvae were washed in ddH_2O and then homogenized in 0.5ml methanol. After centrifugation, the pellet was re-extracted in 0.5ml methanol and then in 0.5ml ethanol. The three supernatants were mixed and 0.5ml was evaporated using a SpeedVac. The pellet was dissolved in 100µl of EIA buffer and subjected to the 20-hydroxyecdysone EIA Kit.

Lifespan analyses

Lifespan analyses was carried out by collecting adult flies 24-36 hours after eclosion and placing flies into vials at a density of 20 animals or fewer. Survival was quantified by transferring flies every two days into vials with fresh food and counting the number of dead animals. Survival analyses were carried out using Log-rank (Mantel-Cox) test in Prism v8.0.

Developmental delay quantification

Female and male flies were placed in a vial and allowed to lay eggs for 16 hours. Starting at day 4 AEL, the number of animals that had pupariated were scored every 24 hours. Pupal genotype was ascertained by balancing *kdm5*^{140} using a CyO-GFP chromosome.

Fertility analyses

To determine fertility, individual female flies were placed in a vial with 5 wild-type male flies and individual males were placed in a vial with 3-5 virgin wild-type females and allowed to mate and lay eggs for 4 days. If larvae were present in the vial by day 5, the fly was designated fertile. In cases where the fly died before day 3 we were unable confidently assess fertility and these animals were eliminated from the analyses.

Image acquisition and processing

Adult fly images were obtained using Zeiss Discovery.V12 SteREO or ZEISS ApoTome microscopes and captured using AxioVision Release 4.8 software. Images of larval tissues were obtained using Zeiss AxioImager.M12 microscope and AxioVision SE64 Release 4.9.1 software. All images were processed using Adobe Photoshop CC 2019.

Statistical analyses

All experiments were done in biological triplicate (minimum) and Ns are provided for each experiment. Fisher's exact test was carried out in R. Student's t-test, one-way ANOVA and Wilcoxen rank-sum tests were carried out using GraphPad Prism.

KEY RESOURCES TABLE

REAGENT or RESOURCE	SOURCE	IDENTIFIER
Antibodies		
KDM5	Secombe lab	(Secombe et al., 2007)
Alpha-tubulin	DSHB	12G10; 1:2000
Phosphorylated ERK	Cell Signaling	9106; 1:250
ERK	Cell Signaling	39763; 1:250
Histone H3	Active Motif	39763; 1:1000
S10 phosphorylated histone H3	Cell Signaling	9701S; 1:1000
Atk	Cell Signaling	9272; 1:200
Dcp-1	Cell Signaling	9578; 1:100
Ser505 phosphorylated Akt	Cell Signaling	4054S; 1:200
Donkey anti-mouse IgG 680RD	LI-COR	925-68072; 1:8000
Donkey anti-rabbit IgG 800CW	LI-COR	926-32213; 1:8000
Alexa Fluro 568 anti-rabbit	Invitrogen	A11036
Alexa Fluor 594 Azide	Invitrogen	A10270
Chemicals, Peptides, and Recombinant Proteins		
Paraformaldehyde	Fisher Scientific	28906
Schneider's Drosophila medium	Fisher Scientific	21720024
20-hydroxyecdysone	Fisher Scientific	H5142
10xPBS	Fisher Scientific	70011069
Trizol	Invitrogen	15596026
Vectashield	Vector Labs	H-1000
Critical Commercial Assays		
Click-IT EdU	Invitrogen	C10337

20-hydroxyecdysone EIA kit	Cayman Chemical	501390
Verso cDNA synthesis kit	Fisher-Thermo	AB-1453
Power SYBR green master mix (real-time PCR)	Fisher-Thermo	4367659
1xNuPAGE LDS sample buffer	Invitrogen	NP0008
4-12% Bis-Tris 1mm gels	Invitrogen	NP0322
PVDF	Fisher Scientific	88518
Experimental Models: Organisms/Strains		
kdm5^{140}	Secombe lab	(Drelon et al., 2018)
wild-type	*kdm5*^{140} ; g[*kdm5*^{WT}:HA]attP-86Fb	(Zamurrad et al., 2018)
w^{1118}	Bloomington Drosophila Stock Center (BDSC)	BL5905
UASp-*kdm5*	Secombe lab	(Secombe et al., 2007)
Ubiquitin-Gal4	BDSC	BL32251
32B-Gal4	BDSC	BL1782
T80-Gal4	BDSC	BL1878
Mai60-Gal4	BDSC	BL30811
spok-Gal4	Michael O'Connor	(Shimell et al., 2018)
phm-Gal4	Michael O'Connor	(Rewitz et al., 2009)
Aug21-Gal4	BDSC	BL20137
Akh-Gal4	BDSC	BL25684
dilp2-Gal4	BDSC	BL37516
CG-Gal4	BDSC	BL7011
Mef2-Gal4	BDSC	BL27390
UAS-torso	Michael O'Connor	(Moeller et al., 2017)
UAS-cD8GFP	BDSC	BL8768
UAS-*cyclin E*	Helena Richardson	(Richardson et al., 1995)
Oligonucleotides		
See Table S1		
Software and Algorithms		
GraphPad v8.0.2	GraphPad Software	N/A
R v3.3.2	http://www.R-project.org/	N/A

Bibliography

Accari, S.L., and Fisher, P.R. (2015). Emerging Roles of JmjC Domain-Containing Proteins. Int Rev Cell Mol Biol *319*, 165-220.

Aggarwal, S.K., and King, R.C. (1969). A comparative study of the ring glands from wild type and 1(2)gl mutant Drosophila melanogaster. J Morphol *129*, 171-199.

Aguila, J.R., Suszko, J., Gibbs, A.G., and Hoshizaki, D.K. (2007). The role of larval fat cells in adult Drosophila melanogaster. The Journal of experimental biology *210*, 956-963.

Albert, M., Schmitz, S.U., Kooistra, S.M., Malatesta, M., Morales Torres, C., Rekling, J.C., Johansen, J.V., Abarrategui, I., and Helin, K. (2013). The histone demethylase Jarid1b ensures faithful mouse development by protecting developmental genes from aberrant H3K4me3. PLoS Genet *9*, e1003461.

Bannister, A.J., and Kouzarides, T. (2011). Regulation of chromatin by histone modifications. Cell Res *21*, 381-395.

Barrett, A., Santangelo, S., Tan, K., Catchpole, S., Roberts, K., Spencer-Dene, B., Hall, D., Scibetta, A., Burchell, J., Verdin, E.*, et al.* (2007). Breast cancer associated transcriptional repressor PLU-1/JARID1B interacts directly with histone deacetylases. Int J Cancer *121*, 265-275.

Benayoun, B.A., Pollina, E.A., Ucar, D., Mahmoudi, S., Karra, K., Wong, E.D., Devarajan, K., Daugherty, A.C., Kundaje, A.B., Mancini, E.*, et al.* (2014). H3K4me3 breadth is linked to cell identity and transcriptional consistency. Cell *158*, 673-688.

Blair, L.P., Cao, J., Zou, M.R., Sayegh, J., and Yan, Q. (2011). Epigenetic Regulation by Lysine Demethylase 5 (KDM5) Enzymes in Cancer. Cancers (Basel) *3*, 1383-1404.

Brookes, E., Laurent, B., Ounap, K., Carroll, R., Moeschler, J.B., Field, M., Schwartz, C.E., Gecz, J., and Shi, Y. (2015). Mutations in the intellectual disability gene KDM5C reduce protein stability and demethylase activity. Hum Mol Genet *24*, 2861-2872.

Cao, J., Liu, Z., Cheung, W.K., Zhao, M., Chen, S.Y., Chan, S.W., Booth, C.J., Nguyen, D.X., and Yan, Q. (2014). Histone demethylase RBP2 is critical for breast cancer progression and metastasis. Cell reports *6*, 868-877.

Catchpole, S., Spencer-Dene, B., Hall, D., Santangelo, S., Rosewell, I., Guenatri, M., Beatson, R., Scibetta, A.G., Burchell, J.M., and Taylor-Papadimitriou, J. (2011). PLU-1/JARID1B/KDM5B is required for embryonic survival and contributes to cell proliferation in the mammary gland and in ER+ breast cancer cells. International journal of oncology *38*, 1267-1277.

Chen, K., Luan, X., Liu, Q., Wang, J., Chang, X., Snijders, A.M., Mao, J.H., Secombe, J., Dan, Z., Chen, J.H.*, et al.* (2019). Drosophila Histone Demethylase KDM5 Regulates Social Behavior through Immune Control and Gut Microbiota Maintenance. Cell Host Microbe *25*, 537-552 e538.

Christesen, D., Yang, Y.T., Somers, J., Robin, C., Sztal, T., Batterham, P., and Perry, T. (2017). Transcriptome Analysis of Drosophila melanogaster Third Instar Larval Ring Glands Points to Novel Functions and Uncovers a Cytochrome p450 Required for Development. G3 (Bethesda) *7*, 467-479.

Collins, B.E., Greer, C.B., Coleman, B.C., and Sweatt, J.D. (2019). Histone H3 lysine K4 methylation and its role in learning and memory. Epigenetics Chromatin *12*, 7.

Cong, B., Ohsawa, S., and Igaki, T. (2018). JNK and Yorkie drive tumor progression by generating polyploid giant cells in Drosophila. Oncogene *37*, 3088-3097.

Danielsen, E.T., Moeller, M.E., and Rewitz, K.F. (2013). Nutrient signaling and developmental timing of maturation. Current topics in developmental biology *105*, 37-67.
Danielsen, E.T., Moeller, M.E., Yamanaka, N., Ou, Q., Laursen, J.M., Soenderholm, C., Zhuo, R., Phelps, B., Tang, K., Zeng, J.*, et al.* (2016). A Drosophila Genome-Wide Screen Identifies Regulators of Steroid Hormone Production and Developmental Timing. Dev Cell *37*, 558-570.
Davoli, T., and de Lange, T. (2011). The causes and consequences of polyploidy in normal development and cancer. Annu Rev Cell Dev Biol *27*, 585-610.
Drelon, C., Belalcazar, H.M., and Secombe, J. (2018). The Histone Demethylase KDM5 Is Essential for Larval Growth in Drosophila. Genetics.
Fox, D.T., and Duronio, R.J. (2013). Endoreplication and polyploidy: insights into development and disease. Development *140*, 3-12.
Frawley, L.E., and Orr-Weaver, T.L. (2015). Polyploidy. Curr Biol *25*, R353-358.
Gajan, A., Barnes, V.L., Liu, M., Saha, N., and Pile, L.A. (2016). The histone demethylase dKDM5/LID interacts with the SIN3 histone deacetylase complex and shares functional similarities with SIN3. Epigenetics Chromatin *9*, 4.
Gaziova, I., Bonnette, P.C., Henrich, V.C., and Jindra, M. (2004). Cell-autonomous roles of the ecdysoneless gene in Drosophila development and oogenesis. Development *131*, 2715-2725.
Gilbert, L.I. (2004). Halloween genes encode P450 enzymes that mediate steroid hormone biosynthesis in Drosophila melanogaster. Mol Cell Endocrinol *215*, 1-10.
Gildea, J.J., Lopez, R., and Shearn, A. (2000). A screen for new trithorax group genes identified little imaginal discs, the Drosophila melanogaster homologue of human retinoblastoma binding protein 2. Genetics *156*, 645-663.
Gu, S.H., Young, S.C., Lin, J.L., and Lin, P.L. (2011). Involvement of PI3K/Akt signaling in PTTH-stimulated ecdysteroidogenesis by prothoracic glands of the silkworm, Bombyx mori. Insect Biochem Mol Biol *41*, 197-202.
Han, M., Xu, W., Cheng, P., Jin, H., and Wang, X. (2017). Histone demethylase lysine demethylase 5B in development and cancer. Oncotarget *8*, 8980-8991.
Howe, F.S., Fischl, H., Murray, S.C., and Mellor, J. (2017). Is H3K4me3 instructive for transcription activation? BioEssays : news and reviews in molecular, cellular and developmental biology *39*, 1-12.
Hrdlicka, L., Gibson, M., Kiger, A., Micchelli, C., Schober, M., Schock, F., and Perrimon, N. (2002). Analysis of twenty-four Gal4 lines in Drosophila melanogaster. Genesis *34*, 51-57.
Iwase, S., Brookes, E., Agarwal, S., Badeaux, A.I., Ito, H., Vallianatos, C.N., Tomassy, G.S., Kasza, T., Lin, G., Thompson, A.*, et al.* (2016). A Mouse Model of X-linked Intellectual Disability Associated with Impaired Removal of Histone Methylation. Cell reports *14*, 1000-1009.
Iwase, S., Lan, F., Bayliss, P., de la Torre-Ubieta, L., Huarte, M., Qi, H.H., Whetstine, J.R., Bonni, A., Roberts, T.M., and Shi, Y. (2007). The X-linked mental retardation gene SMCX/JARID1C defines a family of histone H3 lysine 4 demethylases. Cell *128*, 1077-1088.
Kim, J.H., Lee, J.H., Lee, I.S., Lee, S.B., and Cho, K.S. (2017). Histone Lysine Methylation and Neurodevelopmental Disorders. International journal of molecular sciences *18*.
Klose, R.J., Yan, Q., Tothova, Z., Yamane, K., Erdjument-Bromage, H., Tempst, P., Gilliland, D.G., Zhang, Y., and Kaelin, W.G.J. (2007). The Retinoblastoma binding protein RBP2 is a H3K4 demethylase. Cell *128*, 889-900.

Lee, G., and Park, J.H. (2004). Hemolymph sugar homeostasis and starvation-induced hyperactivity affected by genetic manipulations of the adipokinetic hormone-encoding gene in Drosophila melanogaster. Genetics *167*, 311-323.
Lee, N., Erdjument-Bromage, H., Tempst, P., Jones, R.S., and Zhang, Y. (2009). The H3K4 Demethylase Lid Associates with and Inhibits the Histone Deacetylase Rpd3. Mol Cell Biol *29*, 1401-1410.
Li, L., Greer, C., Eisenman, R.N., and Secombe, J. (2010). Essential functions of the histone demethylase lid. PLoS Genet *6*, e1001221.
Liu, X., Greer, C., and Secombe, J. (2014). KDM5 interacts with Foxo to modulate cellular levels of oxidative stress. PLoS Genet *10*, e1004676.
Liu, X., and Secombe, J. (2015). The Histone Demethylase KDM5 Activates Gene Expression by Recognizing Chromatin Context through Its PHD Reader Motif. Cell reports *13*, 2219-2231.
Lloret-Llinares, M., Perez-Lluch, S., Rossell, D., Moran, T., Ponsa-Cobas, J., Auer, H., Corominas, M., and Azorin, F. (2012). dKDM5/LID regulates H3K4me3 dynamics at the transcription-start site (TSS) of actively transcribed developmental genes. Nucleic Acids Res.
Mariani, L., Lussi, Y.C., Vandamme, J., Riveiro, A., and Salcini, A.E. (2016). The H3K4me3/2 histone demethylase RBR-2 controls axon guidance by repressing the actin-remodeling gene wsp-1. Development *143*, 851-863.
Martin, H.C., Jones, W.D., McIntyre, R., Sanchez-Andrade, G., Sanderson, M., Stephenson, J.D., Jones, C.P., Handsaker, J., Gallone, G., Bruntraeger, M.*, et al.* (2018). Quantifying the contribution of recessive coding variation to developmental disorders. Science.
McBrayer, Z., Ono, H., Shimell, M., Parvy, J.P., Beckstead, R.B., Warren, J.T., Thummel, C.S., Dauphin-Villemant, C., Gilbert, L.I., and O'Connor, M.B. (2007). Prothoracicotropic hormone regulates developmental timing and body size in Drosophila. Dev Cell *13*, 857-871.
McCann, T.S., Sobral, L.M., Self, C., Hsieh, J., Sechler, M., and Jedlicka, P. (2019). Biology and targeting of the Jumonji-domain histone demethylase family in childhood neoplasia: a preclinical overview. Expert Opin Ther Targets, 1-14.
Mirabella, A.C., Foster, B.M., and Bartke, T. (2016). Chromatin deregulation in disease. Chromosoma *125*, 75-93.
Moeller, M.E., Nagy, S., Gerlach, S.U., Soegaard, K.C., Danielsen, E.T., Texada, M.J., and Rewitz, K.F. (2017). Warts Signaling Controls Organ and Body Growth through Regulation of Ecdysone. Curr Biol *27*, 1652-1659 e1654.
Moran, T., Bernues, J., and Azorin, F. (2015). The Drosophila histone demethylase dKDM5/LID regulates hematopoietic development. Dev Biol *405*, 260-268.
Moshkin, Y.M., Kan, T.W., Goodfellow, H., Bezstarosti, K., Maeda, R.K., Pilyugin, M., Karch, F., Bray, S.J., Demmers, J.A., and Verrijzer, C.P. (2009). Histone chaperones ASF1 and NAP1 differentially modulate removal of active histone marks by LID-RPD3 complexes during NOTCH silencing. Mol Cell *35*, 782-793.
Navarro-Costa, P., McCarthy, A., Prudencio, P., Greer, C., Guilgur, L.G., Becker, J.D., Secombe, J., Rangan, P., and Martinho, R.G. (2016). Early programming of the oocyte epigenome temporally controls late prophase I transcription and chromatin remodelling. Nat Commun *7*, 12331.
Nishibuchi, G., Shibata, Y., Hayakawa, T., Hayakawa, N., Ohtani, Y., Sinmyozu, K., Tagami, H., and Nakayama, J. (2014). Physical and functional interactions between the histone H3K4

demethylase KDM5A and the nucleosome remodeling and deacetylase (NuRD) complex. J Biol Chem *289*, 28956-28970.
Niwa, R., and Niwa, Y.S. (2014). Enzymes for ecdysteroid biosynthesis: their biological functions in insects and beyond. Biosci Biotechnol Biochem *78*, 1283-1292.
Ohhara, Y., Kobayashi, S., and Yamanaka, N. (2017). Nutrient-Dependent Endocycling in Steroidogenic Tissue Dictates Timing of Metamorphosis in Drosophila melanogaster. PLoS Genet *13*, e1006583.
Orr-Weaver, T.L. (2015). When bigger is better: the role of polyploidy in organogenesis. Trends Genet *31*, 307-315.
Paroni, G., Bolis, M., Zanetti, A., Ubezio, P., Helin, K., Staller, P., Gerlach, L.O., Fratelli, M., Neve, R.M., Terao, M.*, et al.* (2018). HER2-positive breast-cancer cell lines are sensitive to KDM5 inhibition: definition of a gene-expression model for the selection of sensitive cases. Oncogene.
Plch, J., Hrabeta, J., and Eckschlager, T. (2019). KDM5 demethylases and their role in cancer cell chemoresistance. Int J Cancer *144*, 221-231.
Rewitz, K.F., Yamanaka, N., Gilbert, L.I., and O'Connor, M.B. (2009). The insect neuropeptide PTTH activates receptor tyrosine kinase torso to initiate metamorphosis. Science *326*, 1403-1405.
Richardson, H., O'Keefe, L.V., Marty, T., and Saint, R. (1995). Ectopic cyclin E expression induces premature entry into S phase and disrupts pattern formation in the Drosophila eye imaginal disc. Development *121*, 3371-3379.
Roesch, A., Vultur, A., Bogeski, I., Wang, H., Zimmermann, K.M., Speicher, D., Korbel, C., Laschke, M.W., Gimotty, P.A., Philipp, S.E.*, et al.* (2013). Overcoming Intrinsic Multidrug Resistance in Melanoma by Blocking the Mitochondrial Respiratory Chain of Slow-Cycling JARID1B(high) Cells. Cancer cell *23*, 811-825.
Santos-Rosa, H., Schneider, R., Bannister, A.J., Sherriff, J., Bernstein, B.E., Emre, N.C.T., Schreiber, S.L., Mellor, J., and Kouzarides, T. (2002). Active genes are tri-methylated at K4 of histone H3. Nature *419*, 407-411.
Secombe, J., Li, L., Carlos, L.S., and Eisenman, R.N. (2007). The Trithorax group protein Lid is a trimethyl histone H3K4 demethylase required for dMyc-induced cell growth. Gene Dev *21*, 537-551.
Sharma, K., Singh, J., Frost, E.E., and Pillai, P.P. (2018). MeCP2 in central nervous system glial cells: current updates. Acta Neurobiol Exp (Wars) *78*, 30-40.
Shimell, M., Pan, X., Martin, F.A., Ghosh, A.C., Leopold, P., O'Connor, M.B., and Romero, N.M. (2018). Prothoracicotropic hormone modulates environmental adaptive plasticity through the control of developmental timing. Development *145*.
Tahiliani, M., Mei, P.C., Fang, R., Leonor, T., Rutenberg, M., Shimizu, F., Li, J., Rao, A., and Shi, Y.J. (2007). The histone H3K4 demethylase SMCX links REST target genes to X-linked mental retardation. Nature *447*, 601-+.
Tarayrah, L., Li, Y., Gan, Q., and Chen, X. (2015). Epigenetic regulator Lid maintains germline stem cells through regulating JAK-STAT signaling pathway activity. Biology open *4*, 1518-1527.
Unhavaithaya, Y., and Orr-Weaver, T.L. (2012). Polyploidization of glia in neural development links tissue growth to blood-brain barrier integrity. Genes Dev *26*, 31-36.

Vallianatos, C.N., Farrehi, C., Friez, M.J., Burmeister, M., Keegan, C.E., and Iwase, S. (2018). Altered Gene-Regulatory Function of KDM5C by a Novel Mutation Associated With Autism and Intellectual Disability. Front Mol Neurosci *11*, 104.

Vallianatos, C.N., and Iwase, S. (2015). Disrupted intricacy of histone H3K4 methylation in neurodevelopmental disorders. Epigenomics *7*, 503-519.

Xhabija, B., and Kidder, B.L. (2018). KDM5B is a master regulator of the H3K4-methylome in stem cells, development and cancer. Semin Cancer Biol.

Xiang, J., Bandura, J., Zhang, P., Jin, Y., Reuter, H., and Edgar, B.A. (2017). EGFR-dependent TOR-independent endocycles support Drosophila gut epithelial regeneration. Nat Commun *8*, 15125.

Yamamoto, S., Wu, Z., Russnes, H.G., Takagi, S., Peluffo, G., Vaske, C., Zhao, X., Moen Vollan, H.K., Maruyama, R., Ekram, M.B.*, et al.* (2014). JARID1B is a luminal lineage-driving oncogene in breast cancer. Cancer cell *25*, 762-777.

Yamanaka, N., Rewitz, K.F., and O'Connor, M.B. (2013). Ecdysone control of developmental transitions: lessons from Drosophila research. Annu Rev Entomol *58*, 497-516.

Yamane, K., Tateishi, K., Klose, R.J., Fang, J., Fabrizio, L.A., Erdjument-Bromage, H., Taylor-Papadimitriou, J., Tempst, P., and Zhang, Y. (2007). PLU-1 is a H3K4 demethylase involved in transcriptional repression and breast cancer cell proliferation. Mol Cell *25*, 801-812.

Zamurrad, S., Hatch, H.A.M., Drelon, C., Belalcazar, H.M., and Secombe, J. (2018). A Drosophila Model of Intellectual Disability Caused by Mutations in the Histone Demethylase KDM5. Cell reports *22*, 2359-2369.

Zhaunova, L., Ohkura, H., and Breuer, M. (2016). Kdm5/Lid Regulates Chromosome Architecture in Meiotic Prophase I Independently of Its Histone Demethylase Activity. PLoS Genet *12*, e1006241.

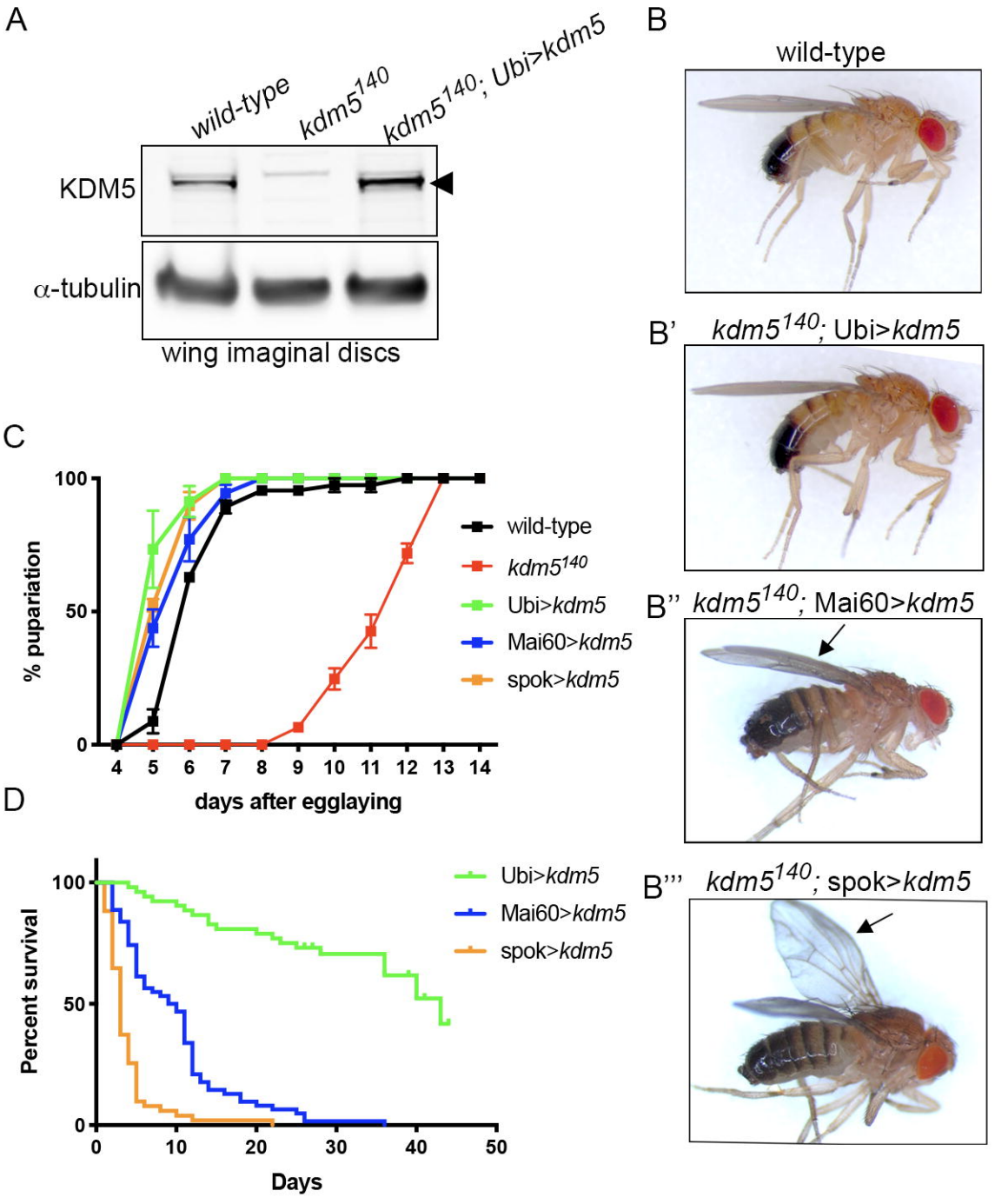
A
wild-type
kdm5140
kdm5140; Ubi>kdm5
KDM5
α-tubulin
wing imaginal discs
B
wild-type
B'
kdm5140; Ubi>kdm5
B''
kdm5140; Mai60>kdm5
B'''
kdm5140; spok>kdm5
C
% pupariation
100
50
0
4 5 6 7 8 9 10 11 12 13 14
days after egglaying
wild-type
kdm5140
Ubi>kdm5
Mai60>kdm5
spok>kdm5
D
Percent survival
100
50
0
0 10 20 30 40 50
Days
Ubi>kdm5
Mai60>kdm5
spok>kdm5

Figure 1

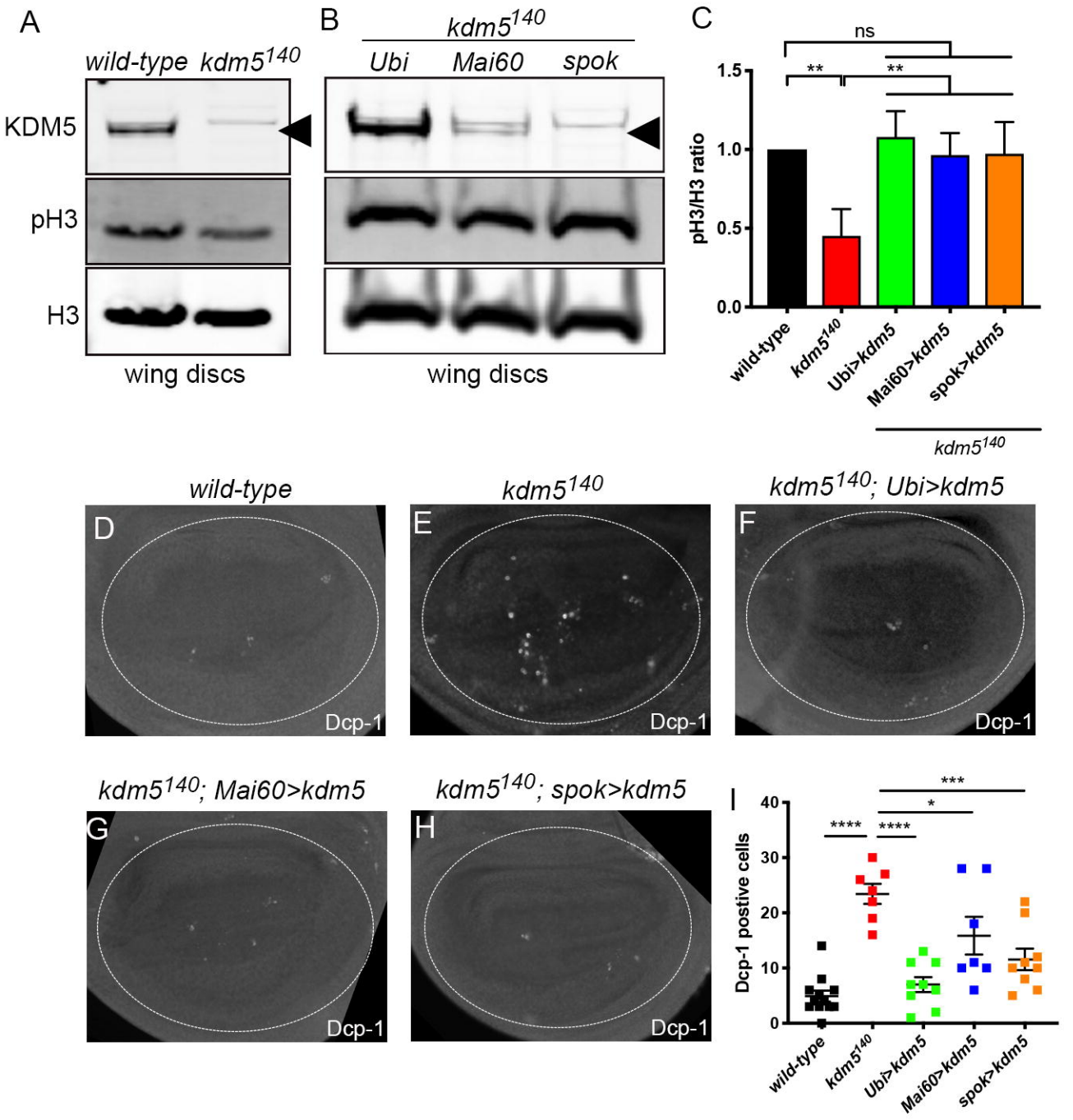
A
wild-type
kdm5140
KDM5
pH3
H3
wing discs
B
kdm5140
Ubi
Mai60
spok
wing discs
C
ns
**
**
pH3/H3 ratio
1.5
1.0
0.5
0.0
wild-type
kdm5140
Ubi>kdm5
Mai60>kdm5
spok>kdm5
kdm5140
wild-type
kdm5140
kdm5140; Ubi>kdm5
D
E
F
Dcp-1
kdm5140; Mai60>kdm5
kdm5140; spok>kdm5
G
H
I
***
*
****
****
Dcp-1 postive cells
40
30
20
10
0
wild-type
kdm5140
Ubi>kdm5
Mai60>kdm5
spok>kdm5

Figure 2

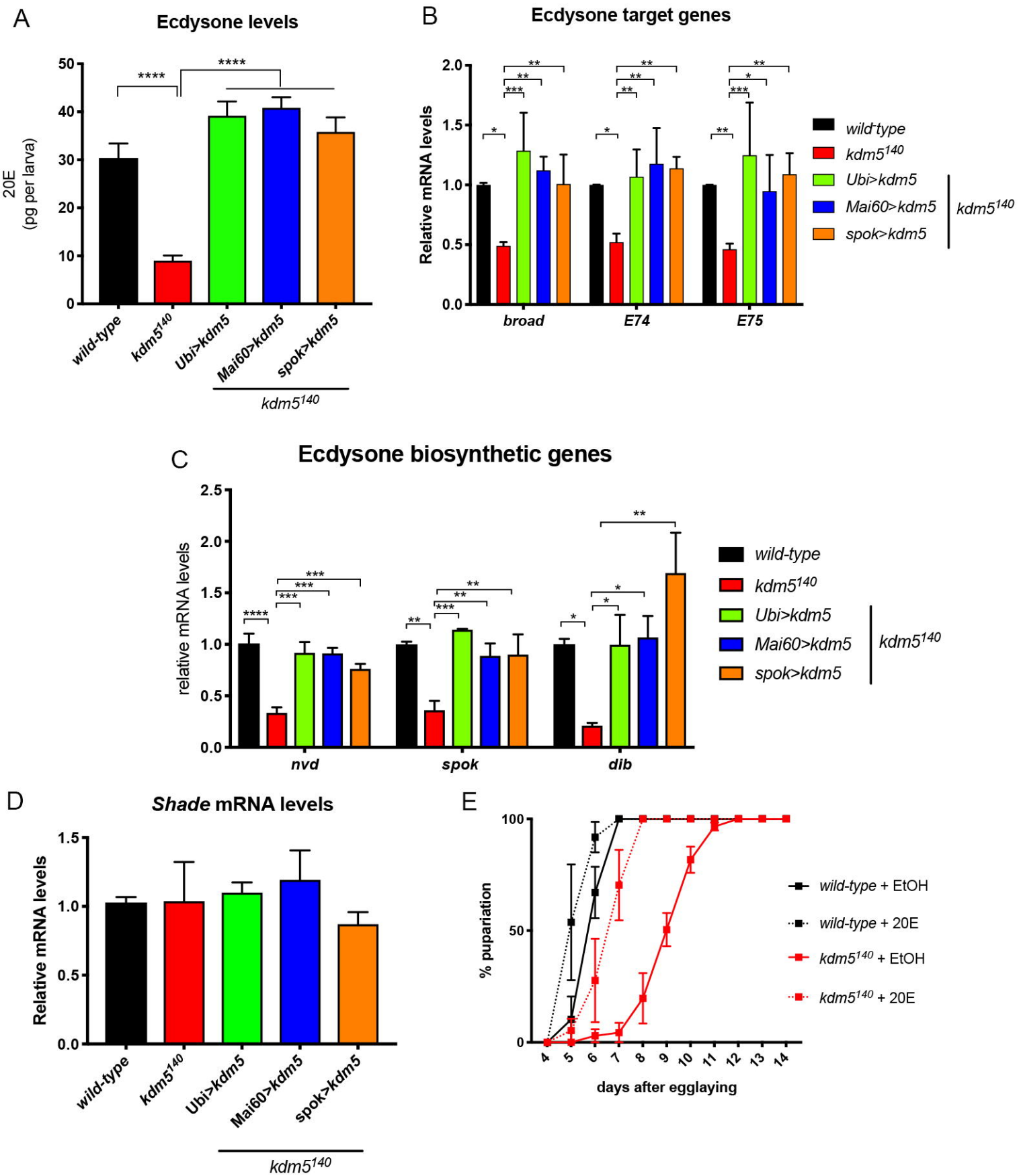
A
Ecdysone levels
20E
(pg per larva)
wild-type
kdm5140
Ubi>kdm5
Mai60>kdm5
spok>kdm5
kdm5140
B
Ecdysone target genes
Relative mRNA levels
broad
E74
E75
wild-type
kdm5140
Ubi>kdm5
Mai60>kdm5
spok>kdm5
kdm5140
C
Ecdysone biosynthetic genes
relative mRNA levels
nvd
spok
dib
wild-type
kdm5140
Ubi>kdm5
Mai60>kdm5
spok>kdm5
kdm5140
D
Shade mRNA levels
Relative mRNA levels
wild-type
kdm5140
Ubi>kdm5
Mai60>kdm5
spok>kdm5
kdm5140
E
% pupariation
days after egglaying
wild-type + EtOH
wild-type + 20E
kdm5140 + EtOH
kdm5140 + 20E

Figure 3

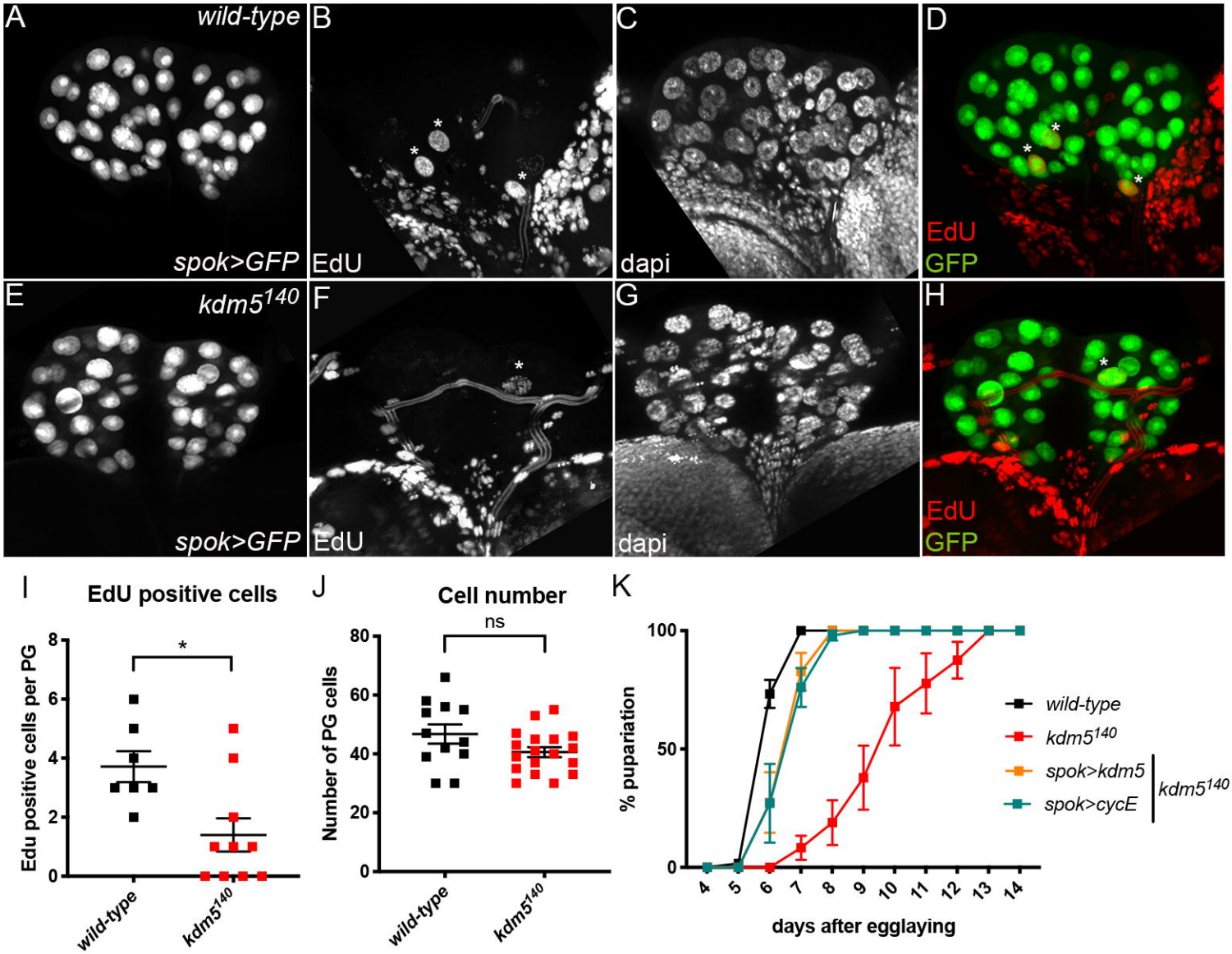
A
wild-type
spok>GFP
B
EdU
C
dapi
D
EdU
GFP
E
kdm5140
spok>GFP
F
EdU
G
dapi
H
EdU
GFP
I
EdU positive cells
Edu positive cells per PG
*
wild-type
kdm5140
J
Cell number
ns
Number of PG cells
wild-type
kdm5140
K
% pupariation
days after egglaying
wild-type
kdm5140
spok>kdm5
spok>cycE
kdm5140

Figure 4

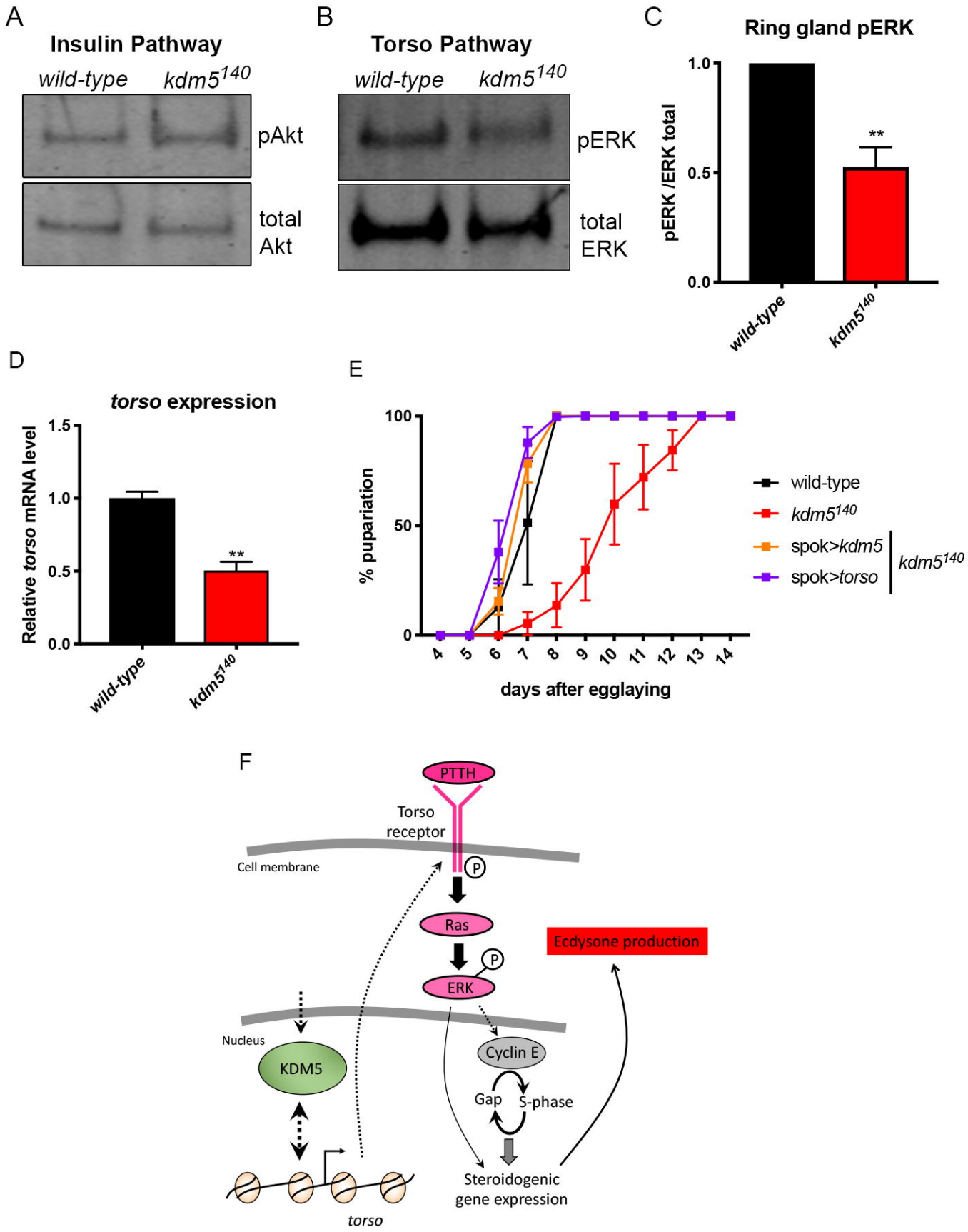
A
Insulin Pathway
wild-type
kdm5140
pAkt
total Akt
B
Torso Pathway
wild-type
kdm5140
pERK
total ERK
C
Ring gland pERK
pERK /ERK total
1.0
0.5
0.0
**
wild-type
kdm5140
D
torso expression
Relative torso mRNA level
1.5
1.0
0.5
0.0
**
wild-type
kdm5140
E
% pupariation
100
50
0
4
5
6
7
8
9
10
11
12
13
14
days after egglaying
wild-type
kdm5140
spok>kdm5
spok>torso
kdm5140
F
PTTH
Torso receptor
Cell membrane
P
Ras
P
ERK
Ecdysone production
Nucleus
KDM5
Cyclin E
Gap
S-phase
Steroidogenic gene expression
torso

Figure 5